Article

Not peer-reviewed version

Exploration of Choroidal Thinning Located Temporally to the Fovea: A Pilot Study

Adèle Ehongo *, Georgina Jawdat De Togme , Viviane De Maertelaer

Posted Date: 12 July 2024

doi: 10.20944/preprints202407.0995.v1

Keywords: Myopia; posterior staphyloma; choroidal thinning; pathogenesis; complication; muscle

Article

Exploration of Choroidal Thinning Located Temporally to the Fovea—A Pilot Study

Adèle Ehongo [1,*], Georgina Jawdat De Togme [2] and Viviane De Maertelaer [3]

[1] Hôpital Universitaire de Bruxelles (HUB), CUB Hôpital Erasme, Service d'Ophtalmologie, route de Lennik 808, 1070 Bruxelles, Belgium
[2] Université Libre de Bruxelles (ULB), route de Lennik 808, 1070 Bruxelles, Belgium ; georgina.jawdat.de.togme@ulb.be
[3] Biostatistics, IRIBHM Université Libre de Bruxelles (ULB), route de Lennik 808, 1070 Bruxelles, Belgium ; viviane.de.maertelaer@ulb.be
* Correspondence: adele.ehongo@hubruxelles.be; Tel +3225553114

Abstract: Background/Objectives: Posterior staphyloma (PS) is a hallmark of pathological myopia corresponding to a circumscribed outpouching of the eyeball with choroidal thinning and inward scleral deformation at its edges. Its pathogenesis is still unclear, thus constituting a research priority as the prevalence of myopia is increasing worldwide. Recently, it has been suggested that the optic nerve sheaths or oblique muscles are potential promoters of PS through the traction or compression effect that they apply to the eye wall. The inferior oblique muscle (IOM) inserts 1-2 mm from the macula. The projection of its insertion is accessible by Optical Coherence Tomography (OCT). Before launching prospective studies, we sought to detect any choroidal thinning (ChT) in the temporal vicinity of the macula and to measure the distance between it and the fovea (FT-distance). **Methods**: This retrospective cross-sectional pilot study included 120 eyes. Using Spectralis-OCT, the area centered by the Bruch's membrane opening-fovea axis was analyzed for ChT and FT-distance. **Results**: Of the 112 defined eyes, 70% (78 eyes) had ChT. Pachymetry was significantly thinner ($p = 0.018$) in eyes with than without ChT. The mean FT-distance was 3601.9 ± 93.6µm. **Conclusion:** The location of ChT coincided with the insertion distance of the IOM, suggesting a link between them. The association between the presence of ChT and thinner pachymetry suggests reduced scleral resistance as thinner pachymetry is related to thinner sclera. Our results support a possible involvement of the IOM in the pathogenesis of certain PS, warranting further investigation.

Keywords: Myopia; posterior staphyloma; choroidal thinning; pathogenesis; complication; muscle

1. Introduction

The strategies currently mobilized against myopia aim to reduce its increasing prevalence as well as the vision-threatening complications linked to this condition. It is estimated that 50% people worldwide will be myopic by 2050, compared to 23% in 2016 [1]. These figures could be revised upwards due to the influence of Covid-19 [2].

Although posterior staphyloma (PS) is one of the main myopic complications leading to poor visual prognosis [3], its pathogenesis is still poorly understood.

Interestingly, it has recently been suggested that peripapillary staphyloma (PPS) results from long-term remodeling and fixation of intermittent eye wall deformations induced by the optic nerve (ON) sheaths on their scleral attachments during eye movements [4,5].

Indeed, traction of the ON sheaths on their scleral insertions during eye movements has been systematically documented by various methods [6–11]. Moreover, the magnitude of this pulling force was quantified to reach that of the extraocular muscles [12].

Therefore, it was hypothesized that oblique muscles which also insert at the back of the globe could potentially favor the appearance of other types of PS, through the same mechanism of sectoral compression and/or traction of the eyeball [13].

 doi:10.20944/preprints202407.0995.v1

As the insertion of the inferior oblique muscle (IOM) is located 1-2 mm from the macula [14], the potential deformations of the eyeball induced by it could be practically evaluated by Optical Coherence Tomography (OCT).

This noninvasive technique is currently established as the gold standard in glaucoma care. It allows to measure the thickness of the different macular layers. With its ability to detect changes from early stage [15] to late-stage disease [16], OCT is a valuable tool for monitoring glaucoma. Macular OCT would even be the latest informative structural tool available to monitor end-stage glaucoma [16,17].

In addition to comprehensive glaucoma diagnostic reports, the Spectralis® Spectral Domain (SD)-OCT provides the 61 frame scans that form the basis of macular analysis, allowing detailed verification of each section if necessary. Finally, the posterior choroidal wall can be visualized in some eyes on OCT scans [18].

The aim of this work was therefore to look for choroidal thinning (ChT) in the temporal vicinity of the macula, using the serial scans constituting the acquisition of posterior pole of Spectralis® OCT. In addition, this study aimed to measure the distance between this potential thinning and the fovea (FT-distance).

2. Materials and Methods

This cross-sectional study was conducted in the glaucoma outpatient department. It complies with the tenets of the Declaration of Helsinki and was approved by the Ethics Committee (reference P2023/423) and the institutional review board (reference SRB2023264).

Records of adult patients who underwent SD-OCT imaging with Spectralis® S3300 model (Heidelberg Engineering GmbH, Heidelberg, Germany) for glaucoma evaluation were retrospectively analyzed. The inclusion was carried out consecutively until 120 eyes were obtained.

Due to the retrospective design, the informed consent was waived. However, for each medical file, the "clinical research" section was checked beforehand, and if the patient had formally objected to the use of their data for study purposes, their wish was respected, and they were not included.

Inclusion criteria**:** good quality OCT imaging and visible posterior choroidal wall. Exclusion criteria: poor quality OCT imaging, non-myopic maculopathy, non-glaucomatous neuropathy, history of trauma, history of glaucoma surgery, history of posterior segment surgery or strabismus surgery. Absence of visibility of the posterior wall of the choroid

2.1. Data Acquisition

2.1.1. General Parameters.

The age and gender of the patients were recorded. For each eye, the refractive error (RE) – spherical equivalent –, visual acuity (LogMar), central corneal thickness (CCT) with Pentacam® (OCULUS Optikgeräte GmbH, Wetzlar, Germany, and the axial length (AL) if present, measured with the IOL master® 700 (Carl Zeiss Meditec AG, Jena, Germany), were recorded. The RE of eyes with a history of refractive surgery or phacoemulsification was not considered.

2.1.2. OCT Analysis.

The OCT and infrared (IR) images were opened in display mode and the following analyses were performed.

- Search for choroidal thinning in 3 locations in the temporal part of the posterior pole.

These measurements were taken at the temporal part respectively: near the fovea, at the upper, and lower limits of the acquisition rectangle. First, the rectangle acquisition band centered by the Bruch's membrane opening-fovea (Fo-BMO) axis and including 10 sections below and 10 sections above this axis was explored (Figure 1A).

 doi:10.20944/preprints202407.0995.v1

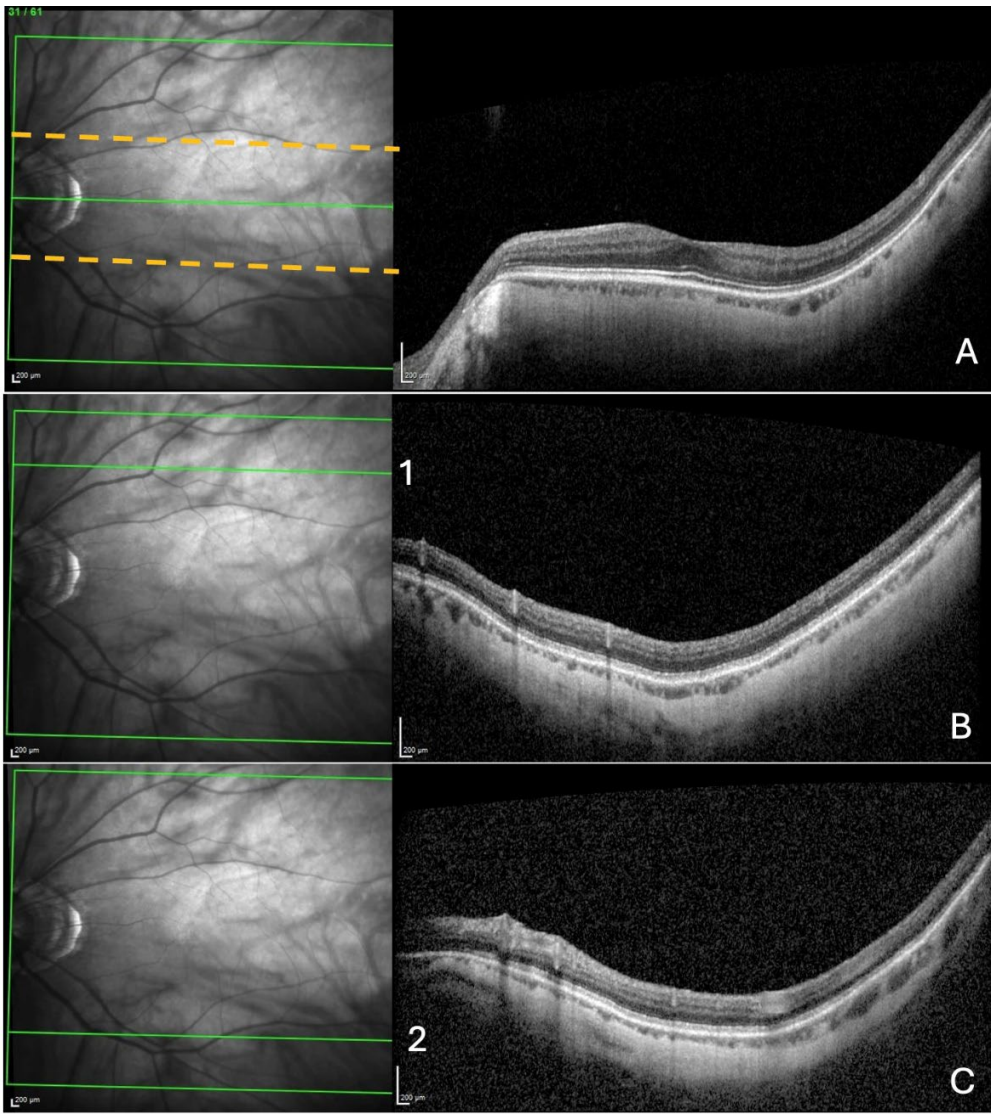

Figure 1. Search for choroidal thinning in 3 locations. 1A. In a band (delineated by the dashed yellow lines) including 10 cross-sections centered by the fovea-Bruch's membrane opening axis. 1B. In the upper limit of acquisition rectangle (10 cross-sections) delineated by line 1. 1C. In the inferior limit of acquisition rectangle (10 cross-sections) delineated by line 2.

The presence of a ChT was sought within this band. Then, from the upper limit of the rectangle acquisition, ten outer sections were analyzed, looking for a choroidal thinning in the same manner as described for the ChT (Figure 1B). Finally, the same procedure was carried out in the inferior part from the lower limit of the acquisition rectangle (Figure 1C).

For each of the three locations, choroidal thinning was considered present when the thinning was noted in at least three adjacent sections (Figures 2A, 2B, 2C), enlarged in (Figures 2D, 2E, 2F).

 doi:10.20944/preprints202407.0995.v1

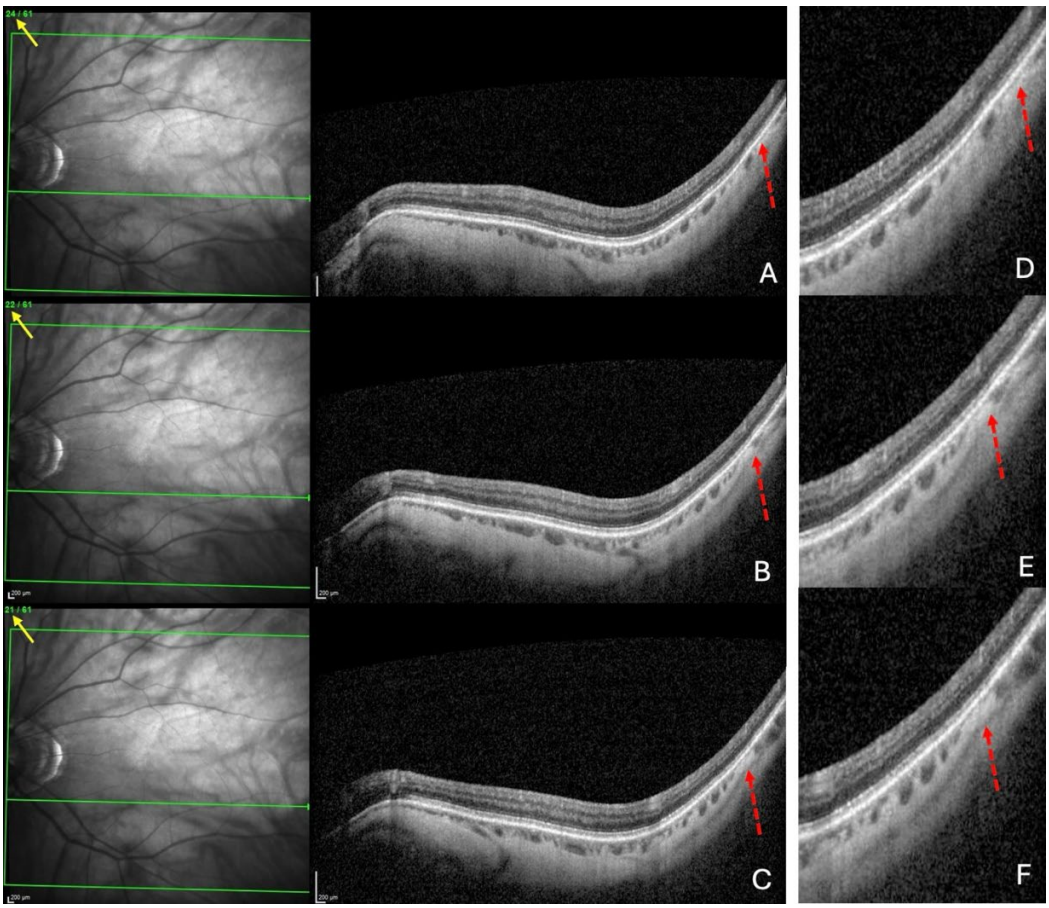

Figure 2. Diagnosis of a choroidal thinning within the band centered by the fovea-Bruch's membrane opening axis. The diagnosis of choroidal thinning was retained if a thinning was noted in at least three consecutive sections (dashed red arrows) in 2A, 2B and 2C, enlarged in 2D, 2E, and 2F. Section numbers are highlighted by the yellow arrows in 2A, 2B and 2C.

- Measurement of the choroidal thinning and distance from fovea to thinning.

For each of the three locations, the measurement of the thinning detected was taken in the section presenting the greatest thinning, at the level of the thinnest part of this choroidal thinning (Figure 3A). The FT-distance was finally measured.

For this purpose, the Early Treatment Diabetic Retinopathy Study (ETDRS) grid was displayed into the IR image and centered on the fovea. The horizontal axis of the ETDRS grid was aligned with the Fo-BMO axis of the OCT image. Then, the OCT line was positioned at the center of the thinning, enabling the visualization of the exact location of the thinning on the IR image (Figure 3B). Finally, the FT-distance on the IR image was measured (Figure 3C). The position of the thinning relative to the Fo-BMO axis (upper, lower or along this axis) was also noted.

All measurements were taken with the Spectralis® built-in caliper tool.

 doi:10.20944/preprints202407.0995.v1

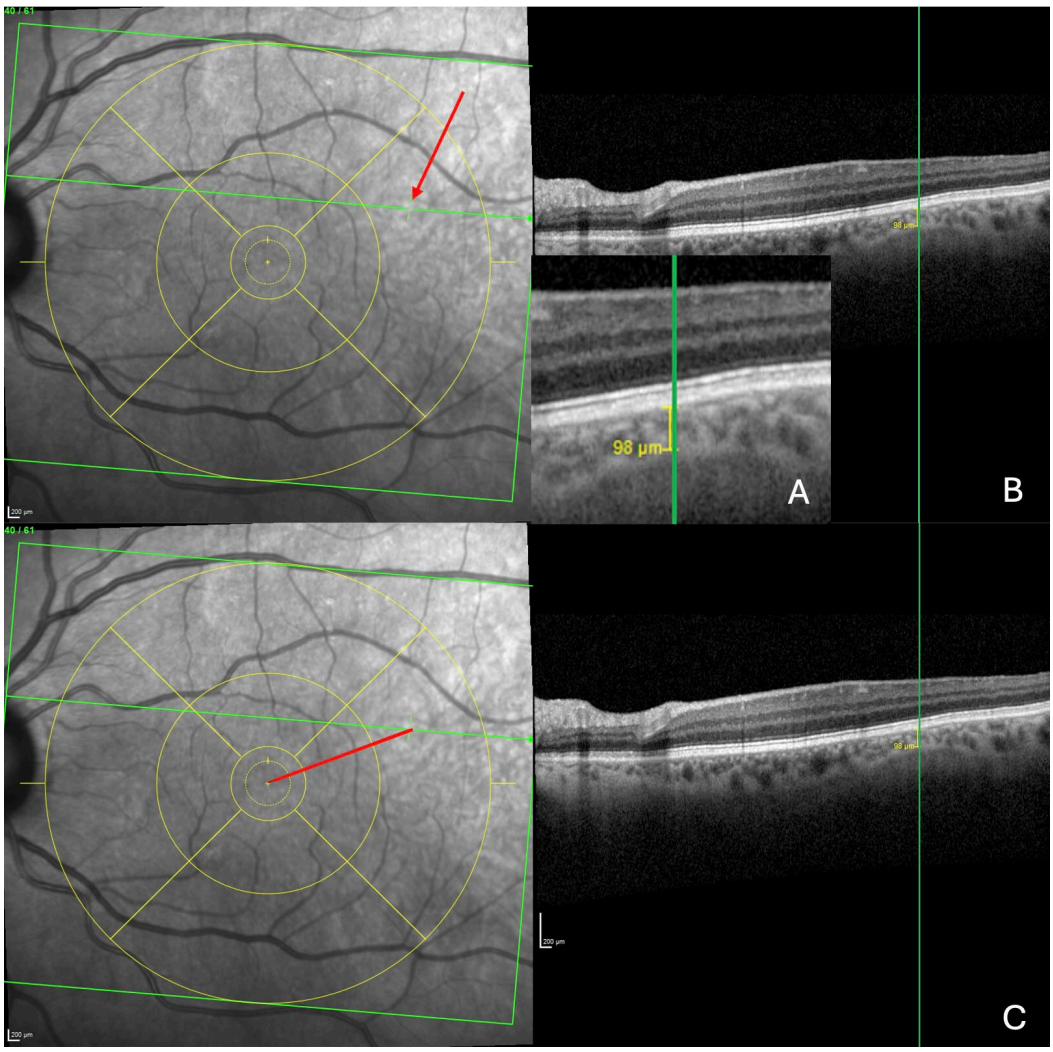

Figure 3. Measurement of the fovea-thinning distance. 3A. The measure of the choroidal thickness is displayed in yellow. 3A is an enlargement of 3B at the location of the thinning. 3B. In the infrared image, the ETDRS grid (yellow circle), is centered on the fovea to facilitate its identification. Then, identification of the thinning on the OCT section (green vertical reference line) is performed. Simultaneously, the location of this thinning is revealed as a discontinuity on the green horizontal reference line (red arrow) at the infrared image. 3C. Measurement of the distance between the fovea and the thinning (red line).

2.2. Analysis Procedure

OCT from all eyes were analyzed independently by two investigators (Ehongo Adèle (EA) and Jawdat De Togme Georgina (JG)).

Before starting the inclusion, the investigators performed a training session on 20 consecutively selected eyes to refine their diagnostic ability. Once prepared, they proceeded to the agreement analysis using 20 other consecutive eyes for which Cohen's kappa statistic was performed for categorical variables, and Pearson and intraclass correlation coefficients for continuous variables. Finally, they moved to the inclusion phase.

They proceeded until the number of included eyes reached 120. The sample size was not estimated beforehand because this is a pilot study.

The mean value of the two examiners' measurements was noted for each variable. In case of disagreement for a variable, the mention undefined was noted for this variable.

 doi:10.20944/preprints202407.0995.v1

2.3. Statistical Analyses.

All the undefined data were excluded from analyses. Descriptive statistics were presented as mean, median, standard deviation or SEM, and range for continuous variables, proportions and percentages for discrete variables.

Relationships between the presence of ChT and the other variables were assessed. Discrete variables were compared using Fisher's exact test. The comparison analyses were performed using ANOVA, followed by Tukey post-hoc analysis and Pearson's correlations. The IBM-SPSS V28.0 statistical software was used. A p-value lower than 0.05 was considered statistically significant.

3. Results

3.1. Analysis of inter-Observer Agreement.

The inter-observer analysis performed on 20 eyes showed excellent agreement for the 5 continuous variables. Pearson correlation coefficients ranged from 0.995 to 0.997 and intraclass correlation coefficients ranged from 0.997 to 1. All were statistically significant ($p<0.001$) (**Table S1**).

Additionally, for the categorical variable (the presence of choroidal thinning), there was a strong inter-observer agreement among the raters, evidenced by a Cohen's Kappa coefficient of 1, also with statistical significance ($p<0.001$).

3.2. Characteristics of the Sample Population.

Overall, 120 eyes of 70 subjects were included, 44 (62%) of whom were females. The mean age ± standard deviation was 69.5 ± 9.8 years, range (41–90). The demographic and ocular features of the sample population are summarized in **Table 1**. A history of refractive surgery or phacoemulsification was found in 41 eyes from which refractive data were therefore excluded.

Table 1. Demographic and ocular characteristics of the study sample: 120 eyes of 70 subjects.

Parameter	*Sample size (n)*	*Mean ± SD*	*Range*
Age (years)	70	69.5 ± 9.8	41 – 90
Refraction (Diopter)	79	-0.14 ± 2.6	-8, 5.4
Pachymetry (µm)	118	554.7 ± 40.5	452 – 662
Axial length (mm)	46	23.9 ± 1.6	19.5 – 27.8

Note: The sample size for each variable corresponds to the number of eyes for which the variable was found in the file. Missing data result from the retrospective design of the study.

3.3. Analysis of Choroidal Thinning at 3 Temporal Sites Relative to the Axis Vertically Aligned with the Fovea

The prevalence of thinning in each of the three temporal choroidal locations explored is presented in **table 2**. For ChT, 112 eyes were defined. It was found in 69.6 % (78/112 eyes) of them and was significantly more frequent than lower or upper thinnings, ($p< 0.001$) in both cases.

Table 2. Prevalence of choroidal thinning in the 3 sites of the acquisition rectangle.

Location	**Sample size (n)**	**Present (n)**	**Proportion %**
Upper part of rectangle	109	25	22.9
Part centered by the Fo-BMO axis	112	78	69.6
Lower part of rectangle	114	29	25.4

Note: The sample size for each variable corresponds to the number of eyes defined for that variable. The proportion of choroidal thinning (Fisher exact test) was significantly different in the zone centered by the Fo-

 doi:10.20944/preprints202407.0995.v1

BMO axis than in the superior ($p < 0.001$) or inferior positions ($p < 0.001$). Abbreviation: Fo-BMO = fovea-Bruch's membrane opening.

3.4. Detailed Analysis of Choroidal Thinning at the Vicinity of the Fo-BMO Axis (ChT)

The mean thickness of the ChT (mean ± SD) at its thinnest part was 107.8 ± 6.9 µm, with a range of 9-254 µm.

The distribution of ChT relative to the Fo-BMO axis is shown in **Table 3.** Although the proportion of eyes with ChT below the Fo-BMO axis was higher than that along the Fo-BMO axis or superior to the Fo-BMO axis, this was not statistically significant, respectively (p = 0,093 and 0,133).

Table 3. Distribution of ChT around the Fo-BMO axis.

Proportions of ChT around the Fo-BMO axis			
Location	Sample size (n)	Present (n)	Proportion %
Superior location	78	23	29.5
Along the Fo-BMO axis	78	22	28.5
Inferior location	78	33	42.3

Note: There was no significant difference in the prevalence of ChT around the Fo-BMO axis. Abbreviation: ChT = choroidal thinning centered by the Fo-BMO axis. Fo-BMO = fovea-Bruch's membrane opening.

The mean CCT was significantly ($p = 0.018$) thinner in eyes with than without a ChT (549.7 ± 37.8 µm versus 569.1 ± 42.2 µm). All other variables (age, gender, AL and FT-distance) showed no significant association with ChT.

3.5. Analysis of the Distance ChT – Fovea (FT-Distance)

The mean FT-distance value was 3601.9 ± 93.6 µm (mean ± SD), with a range of 1259-5171 µm **(Table 4).**

Table 4. Distance between ChT and fovea (FT- distance) according to the Fo-BMO axis.

Location	*Sample size (n)*	*Mean ± SD*	*Range*
Overall (µm)	78	3601.9 ± 93.6	1259 – 5171
Superior (µm)	23	3201.7 ± 163.5	1530 – 4373
Along FoBMO axis (µm)	22	3544.6 ± 165.5	1477 – 4587
Inferior (µm)	33	3918.9 ± 135.3	1259 – 5171

Note: The FT-distance was longer below compared to above the Fo-BMO axis ($p = 0.003$). Abbreviation: Fo-BMO = fovea-Bruch's membrane opening. FT-distance = distance between the fovea and the ChT. ChT = choroidal thinning centered by the fovea-Bruch's membrane opening axis.

The FT-distance was significantly ($p = 0.003$) longer when the ChT was located below than above the Fo-BMO axis (3918.9 ± 135.3 µm versus 3201.7 ± 163.5 µm).

Longer AL were significantly ($p = 0.047$) associated with longer FT-distance **(Figure 4).**

 doi:10.20944/preprints202407.0995.v1

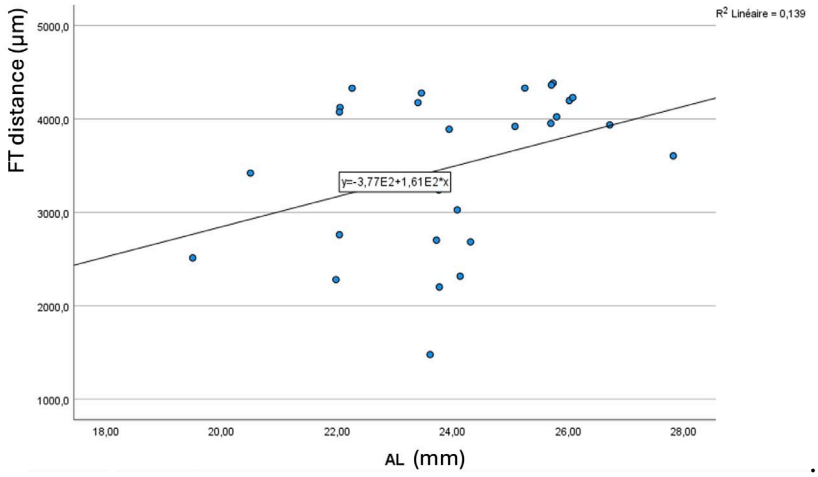

Figure 4. Correlation between the fovea-thinning distance and the axial length.

Abbreviation. FT = fovea-thinning distance. AL = axial length.

All other variables (age, gender, and CCT) showed no significant association with FT-distance.

4. Discussion

Predictions regarding myopia are on the rise worldwide [1]. Its complications have a poor prognosis [3] and explain efforts to slow their progression. This requires a better understanding of their pathogenesis. Unfortunately, many unknowns remain.

Recent ocular biomechanics data have systematically shown that forces acting on the eye wall during eye movements are relevant [7,12] and could contribute to the genesis of certain myopic complications [4,5,7,8,12,13,19].

Particularly, it has been suggested that PS could result from these mechanisms [4,5,13].

In the past, it was assumed that the protrusion of the eyeball characterizing PS resulted from pushing forces directed from inside the eye toward the eye wall [3,20–22]. The idea of a traction force acting from the outside has never been put forward and has just been suggested very recently, first for PPS [4,5], then for other types of PS [13].

Based on OCT, a PS is defined by an outward protrusion of the sclera ending at its edges in an inward scleral deformation. In addition, the choroid thins towards the edge of the PS and re-thickens towards the outpouching of the PS [23,24].

Thinning of the choroid due to compressive force applied to the sclera has been previously documented [8,25]. This thinning is followed by a re-thickening at the limits of the compressed zone. It has also been suggested that the choroid thickens where the sclera is pulled outward [4,5,13] because Bruch's membrane, thanks to its resistance tends to maintain its plane [26].

From this, it was suggested that the underlying pathogenesis of some PS involves inward scleral deformation by compression forces and its outward deformation by traction forces [4,5,13] applied by ON sheaths [4,5] or oblique muscles [13]. The repetition of these deformations over time would lead to remodeling and fixation of the tissues in the deformed configuration [4,5,13] (**Figure 5**).

 doi:10.20944/preprints202407.0995.v1

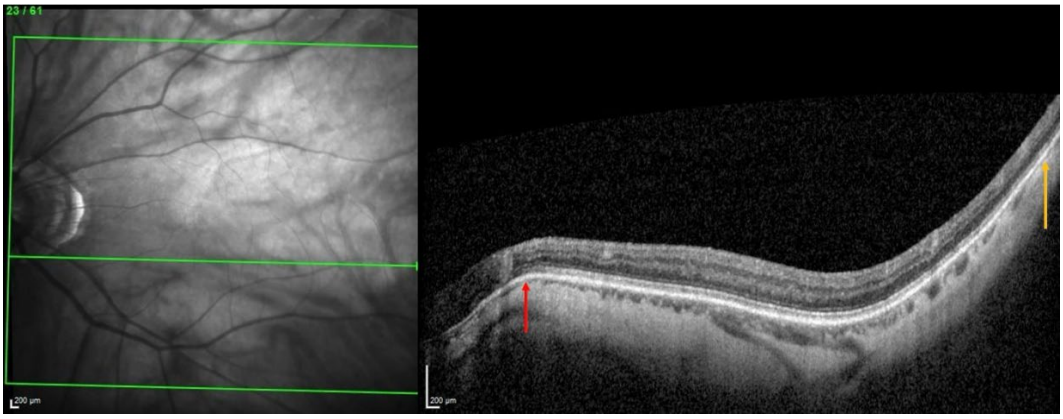

Figure 5. Illustration of two choroidal thinnings related to scleral inward deformations. The choroidal thinning at the peripapillary zone (red arrow) would result from squeezing by the optic nerve sheaths, while the other thinning, temporal to macular position (yellow arrow) would be related to the action of the inferior oblique muscle.

To explore this hypothesis, and before moving on to prospectives studies, we first sought to look for a ChT near and temporal to the macula. Our results revealed a ChT in 70% of eyes, supporting our hypothesis of potential compressive forces at this location in some eyes.

The second unprecedented result came from correlation analyses showing that a thinner CCT was significantly associated with the presence of ChT. As previous results have found a positive correlation between CCT and scleral thickness [27], we suggest that eyes with thinner CCT, and therefore thinner scleral thickness, would also exhibit lower scleral stiffness which would favor local areas of choroidal thinning when the eye wall is subjected to mechanical compression. It is well-known that PS in myopia is favored by reduced scleral rigidity resulting from scleral thinning and remodeling during myopic elongation [20].

Our second objective was to measure the FT-distance. This distance was 3601.9 ± 93.6µm (means ± SD), range 1259 to 5171 µm, meaning that the ChT was positioned 1-5 mm temporal to the fovea, thus coinciding with the insertion distance of the IOM, and supporting our hypothesis.

Interestingly, we found a positive correlation between the FT-distance and the AL, indicating that an elongated eyeball would keep thinning away from the fovea, because the insertion of IOM on the eye is fixed while the part of eye between the ON and this insertion lengthens. This is consistent with previous results showing that the fovea-optic disc distance is positively correlated with AL [28].

Finally, our results showed that the FT-distance was significantly longer when the ChT was located below than above the Fo-BMO axis. We suggest that this is related to the path of the IOM along the eye. From its origin at the orbital floor, the IOM runs on the inferior surface of the eye and finally inserts on the posterior inferolateral surface of the eye [14]. This path may present variability, therefore leading to variability of scleral insertion.

So, just like the perimeter of a curve (the path of the IOM along the eye), from the same starting point (origin of the IOM), for the same length (the length of the IOM), the path with a longer radius of curvature would end (scleral insertion of the IOM) before (below the Fo-BMO axis) the one with the smaller radius of curvature (above the Fo-BMO axis). Additionally, as mentioned above, in the presence of a longer AL, the IOM length is partly depleted by eye elongation, compared to a shorter AL.

Limitations and Perspectives

This study is a retrospective investigation and therefore has several inherent limitations. Furthermore, as this is a pilot investigation, and the potential action of the IOM applies to all eyes, we chose to include eyes consecutively, provided that the posterior choroidal wall was visible. We did not specifically analyze the impact of myopia or PS to avoid the risk of bias by using post-acquisition definition of either entity. The prevalence of ChT is expected to be higher in these groups

 doi:10.20944/preprints202407.0995.v1

of eyes. Therefore, prospective studies which would specify clearly the definition of each entity (myopia and PS) are warranted.

Interestingly, our results support the hypothesis we formulated and pave the way for potential prospective studies that overcome the limitations of the present study.

First, its retrospective nature led to some missing data. Second, the posterior pole module of Spectralis ® that we used would have missed ChT located outside the acquisition rectangle. Third, the analysis we performed is extremely simplistic because it neglects other factors that obviously interact. Finally, potential interactions could evolve over time depending on the progression of myopia and its degenerative changes.

5. Conclusions

This pilot study revealed a ChT in 70% of eyes. The CCT was significantly thinner in eyes with than without ChT. The FT-distance was the same value as the IOM insertion distance from the macula. This FT-distance was positively correlated with the AL and was longer in eyes with a ChT positioned below the Fo-BMO axis.

These results provide new information to explore a potential link between the impact of the IOM and certain PS, warranting further investigation.

Supplementary Materials: Table S1 can be downloaded at the website of this paper posted on Preprints.org..

Table S1. Inter-observer agreement between two readers for 5 continuous variables and n = 20 eyes.

Parameter	Reader	Mean ± SD (µm)	Intra-class correlation	Range (95% confidence interval)	*p-value*
Superior thickness (n = 20)	R1	210.1 ± 91.9	0.998	0.995 - 0.999	*<0.001*
	R2	207.5 ± 92.7			
Inferior thickness (n = 20)	R1	157.3 ± 77.6	0.998	0.996 - 0.999	*<0.001*
	R2	157 ± 76.7			
Retro-foveal (n = 20)	R1	182.1 ± 77.5	0.997	0.993 – 0.999	*<0.001*
	R2	180.9 ± 74.7			
Thickness of thinning (n = 13)	R1	96.9 ± 49.2	0.998	0.994 – 0.999	*<0.001*
	R2	96. ± 47.4			
Distance fovea-thinning (n = 13)	R1	3465.1 ± 755.8	0.998	0.995 – 1.000	*<0.001*
	R2	3461.2 ± 766.8			

Note: R1 = Reader 1 = AE. R2 = Reader 2 = JG.

Author Contributions: Conceptualization, A.E. and G.J.; methodology, A.E. and G.J.; validation, NA.; formal analysis, A.E.; G.J. and VDM.; investigation, A.E. and G.J.; statistics: VDM.; resources, NA; data curation, A.E.; G.J. and VDM.; writing—original draft preparation. A.E.; writing—review and editing, A.E.; G.J. and VDM; visualization, NA; supervision, NA; project administration, NA.; funding acquisition, NA. All authors have read and agreed to the published version of the manuscript.

Funding: This research received no external funding.

Institutional Review Board Statement: The study was conducted in accordance with the Declaration of Helsinki and was approved by the Institutional Review Board (reference SRB2023264) and Ethics Committee (reference P2023/423) of HUB, Erasme Hospital, Brussels.

Informed Consent Statement: Patient consent was waived due to the retrospective design of this analysis.

Data Availability Statement: The data presented in this study are available on request from the corresponding author due to privacy and ethical restrictions.

Acknowledgments: The authors would like to thank Maurine Salmon, Biomedical Research Department, HUB Erasme Hospital, for advice in biostatistics.

Conflicts of Interest: The authors declare no conflicts of interest.

References

1. Holden BA, Fricke TR, Wilson DA, Jong M, Naidoo KS, Sankaridurg P, Wong TY, Naduvilath TJ, Resnikoff S. Global Prevalence of Myopia and High Myopia and Temporal Trends from 2000 through 2050. Ophthalmology. 2016 May;123(5):1036-42. doi: 10.1016/j.ophtha.2016.01.006. Epub 2016 Feb 11. PMID: 26875007.
2. Luo Z, Guo C, Yang X, Zhang M. Comparison of myopia progression among Chinese schoolchildren before and during COVID-19 pandemic: a meta-analysis. Int Ophthalmol. 2023 Oct;43(10):3911-3921. doi: 10.1007/s10792-023-02777-0. Epub 2023 Jun 30. PMID: 37389764.
3. Ohno-Matsui K, Jonas JB. Posterior staphyloma in pathologic myopia. Prog Retin Eye Res. 2019 May;70:99-109. doi: 10.1016/j.preteyeres.2018.12.001. Epub 2018 Dec 8. PMID: 30537538.
4. Ehongo A, Bacq N, Kisma N, Dugauquier A, Alaoui Mhammedi Y, Coppens K, Bremer F, Leroy K. Analysis of Peripapillary Intrachoroidal Cavitation and Myopic Peripapillary Distortions in Polar Regions by Optical Coherence Tomography. Clin Ophthalmol. 2022 Aug 13;16:2617-2629. doi: 10.2147/OPTH.S376597. PMID: 35992567; PMCID: PMC9387167.
5. Ehongo A, Bacq N. Peripapillary Intrachoroidal Cavitation. J Clin Med. 2023 Jul 16;12(14):4712. doi: 10.3390/jcm12144712. PMID: 37510829; PMCID: PMC10380777.
6. Demer JL. Optic Nerve Sheath as a Novel Mechanical Load on the Globe in Ocular Duction. Invest Ophthalmol Vis Sci. 2016 Apr;57(4):1826-38. doi: 10.1167/iovs.15-18718. PMID: 27082297; PMCID: PMC4849549.
7. Wang X, Beotra MR, Tun TA, Baskaran M, Perera S, Aung T, Strouthidis NG, Milea D, Girard MJ. In Vivo 3-Dimensional Strain Mapping Confirms Large Optic Nerve Head Deformations Following Horizontal Eye Movements. Invest Ophthalmol Vis Sci. 2016 Oct 1;57(13):5825-5833. doi: 10.1167/iovs.16-20560. PMID: 27802488.
8. Chang MY, Shin A, Park J, Nagiel A, Lalane RA, Schwartz SD, Demer JL. Deformation of Optic Nerve Head and Peripapillary Tissues by Horizontal Duction. Am J Ophthalmol. 2017 Feb;174:85-94. doi: 10.1016/j.ajo.2016.10.001. Epub 2016 Oct 15. PMID: 27751810; PMCID: PMC5812679.
9. Suh SY, Clark RA, Demer JL. Optic Nerve Sheath Tethering in Adduction Occurs in Esotropia and Hypertropia, But Not in Exotropia. Invest Ophthalmol Vis Sci. 2018 Jun 1;59(7):2899-2904. doi: 10.1167/iovs.18-24305. PMID: 30025141; PMCID: PMC5989862.
10. Lee WJ, Kim YJ, Kim JH, Hwang S, Shin SH, Lim HW. Changes in the optic nerve head induced by horizontal eye movements. PLoS One. 2018 Sep 18;13(9):e0204069. doi: 10.1371/journal.pone.0204069. Erratum in: PLoS One. 2019 May 9;14(5):e0216861. PMID: 30226883; PMCID: PMC6143247.
11. Clark RA, Suh SY, Caprioli J, Giaconi JA, Nouri-Mahdavi K, Law SK, Bonelli L, Coleman AL, Demer JL. Adduction-Induced Strain on the Optic Nerve in Primary Open Angle Glaucoma at Normal Intraocular Pressure. Curr Eye Res. 2021 Apr;46(4):568-578. doi: 10.1080/02713683.2020.1817491. Epub 2020 Sep 11. PMID: 32911989; PMCID: PMC7947028.
12. Wang X, Fisher LK, Milea D, Jonas JB, Girard MJ. Predictions of Optic Nerve Traction Forces and Peripapillary Tissue Stresses Following Horizontal Eye Movements. Invest Ophthalmol Vis Sci. 2017 Apr 1;58(4):2044-2053. doi: 10.1167/iovs.16-21319. PMID: 28384725.
13. Ehongo A. Understanding Posterior Staphyloma in Pathologic Myopia: Current Overview, New Input, and Perspectives. Clin Ophthalmol. 2023 Dec 12;17:3825-3853. doi: 10.2147/OPTH.S405202. PMID: 38105912; PMCID: PMC10725704.
14. Gupta N, Patel BC. Anatomy, Head and Neck: Eye Inferior Oblique Muscles. 2023 Jul 25. In: StatPearls [Internet]. Treasure Island (FL): StatPearls Publishing; 2024 Jan–. PMID: 31424837.
15. Mehta B, Ranjan S, Sharma V, Singh N, Raghav N, Dholakia A, Bhargava R, Reddy PLS, Bargujar P. The Discriminatory Ability of Ganglion Cell Inner Plexiform Layer Complex Thickness in Patients with Preperimetric Glaucoma. J Curr Ophthalmol. 2024 Mar 29;35(3):231-237. doi: 10.4103/joco.joco_124_23. PMID: 38681693; PMCID: PMC11047817.
16. Shin JW, Sung KR, Lee GC, Durbin MK, Cheng D. Ganglion Cell-Inner Plexiform Layer Change Detected by Optical Coherence Tomography Indicates Progression in Advanced Glaucoma. Ophthalmology. 2017 Oct;124(10):1466-1474. doi: 10.1016/j.ophtha.2017.04.023. Epub 2017 May 23. PMID: 28549518.
17. Sung MS, Heo H, Park SW. Structure-function Relationship in Advanced Glaucoma After Reaching the RNFL Floor. J Glaucoma. 2019 Nov;28(11):1006-1011. doi: 10.1097/IJG.0000000000001374. PMID: 31567911.
18. Meng LH, Yuan MZ, Zhao XY, Yu WH, Chen YX. Wide-field swept source optical coherence tomography evaluation of posterior segment changes in highly myopic eyes. Eur J Ophthalmol. 2022 Sep;32(5):2777-2788. doi: 10.1177/11206721211062362. Epub 2021 Nov 29. PMID: 34841931.
19. Ehongo A, Hasnaoui Z, Kisma N, Alaoui Mhammedi Y, Dugauquier A, Coppens K, Wellens E, de Maertelaere V, Bremer F, Leroy K. Peripapillary intrachoroidal cavitation at the crossroads of peripapillary myopic changes. Int J Ophthalmol. 2023 Dec 18;16(12):2063-2070. doi: 10.18240/ijo.2023.12.20. PMID: 38111938; PMCID: PMC10700091.

20. McBrien NA, Gentle A. Role of the sclera in the development and pathological complications of myopia. Prog Retin Eye Res. 2003 May;22(3):307-38. doi: 10.1016/s1350-9462(02)00063-0. PMID: 12852489.
21. Ohno-Matsui K, Akiba M, Modegi T, Tomita M, Ishibashi T, Tokoro T, Moriyama M. Association between shape of sclera and myopic retinochoroidal lesions in patients with pathologic myopia. Invest Ophthalmol Vis Sci. 2012 Sep 7;53(10):6046-61. doi: 10.1167/iovs.12-10161. PMID: 22879412.
22. Jonas JB, Jonas RA, Bikbov MM, Wang YX, Panda-Jonas S. Myopia: Histology, clinical features, and potential implications for the etiology of axial elongation. Prog Retin Eye Res. 2023 Sep;96:101156. doi: 10.1016/j.preteyeres.2022.101156. Epub 2022 Dec 28. PMID: 36585290.
23. Shinohara K, Moriyama M, Shimada N, Yoshida T, Ohno-Matsui K. Characteristics of Peripapillary Staphylomas Associated With High Myopia Determined by Swept-Source Optical Coherence Tomography. Am J Ophthalmol. 2016 Sep;169:138-144. doi: 10.1016/j.ajo.2016.06.033. Epub 2016 Jun 27. PMID: 27365146.
24. Shinohara K, Shimada N, Moriyama M, Yoshida T, Jonas JB, Yoshimura N, Ohno-Matsui K. Posterior Staphylomas in Pathologic Myopia Imaged by Widefield Optical Coherence Tomography. Invest Ophthalmol Vis Sci. 2017 Jul 1;58(9):3750-3758. doi: 10.1167/iovs.17-22319. PMID: 28738419.
25. Chen JY, Le A, De Andrade LM, Goseki T, Demer JL. Compression of the Choroid by Horizontal Duction. Invest Ophthalmol Vis Sci. 2019 Oct 1;60(13):4285-4291. doi: 10.1167/iovs.19-27522. PMID: 31618765.
26. Wang X, Teoh CKG, Chan ASY, Thangarajoo S, Jonas JB, Girard MJA. Biomechanical Properties of Bruch's Membrane-Choroid Complex and Their Influence on Optic Nerve Head Biomechanics. Invest Ophthalmol Vis Sci. 2018 Jun 1;59(7):2808-2817. doi: 10.1167/iovs.17-22069. PMID: 30029276.
27. Sung MS, Ji YS, Moon HS, Heo H, Park SW. Anterior Scleral Thickness in Myopic Eyes and Its Association with Ocular Parameters. Ophthalmic Res. 2021;64(4):567-576. doi: 10.1159/000512396. Epub 2020 Oct 20. PMID: 33080596.
28. Jonas RA, Wang YX, Yang H, Li JJ, Xu L, Panda-Jonas S, Jonas JB. Optic Disc-Fovea Distance, Axial Length and Parapapillary Zones. The Beijing Eye Study 2011. PLoS One. 2015 Sep 21;10(9):e0138701. doi: 10.1371/journal.pone.0138701. PMID: 26390438; PMCID: PMC4577126.